

## MEASUREMENT OF THE ATTACHMENT OF SLOW ELECTRONS IN OXYGEN\*

L. M. Chanin, A. V. Phelps, and M. A. Biondi  
Westinghouse Research Laboratories, Pittsburgh, Pennsylvania  
(Received March 20, 1959)

The study of electron attachment in oxygen has been the subject of numerous investigations,<sup>1-6</sup> and is currently of great interest in connection with upper atmosphere research. In general, the measurements have been interpreted in terms of two-body attachment processes for electron energies ranging from thermal (0.04 eV) to tens of electron volts. The present measurements extend drift tube measurements into the thermal energy range where they are compared with microwave afterglow results<sup>5</sup> and give evidence that at low electron energies (<1 eV) the attachment occurs by a three-body process.

The present method is similar in principle to that used by Doehring.<sup>2</sup> A pulse of electrons is liberated from a photocathode and drifts in a uniform electric field to a collector electrode. A shutter grid<sup>6</sup> near the collector is used to control the flow of electrons and ions to the collector. The time at which the shutter is opened can be delayed with respect to the electron pulse in order to observe the time dependence of the negative-ion arrival at the collector.

If the electron attachment probability per unit drift distance in the field is  $\alpha$ , then the decrease in electron density,  $n_e$ , in the pulse while moving a distance,  $dx$ , in the field direction is  $dn_e = -\alpha n_e dx$ . From this it can be shown that the arrival of ions at the collector is described by

$$N_i = N_i(0) \exp(\alpha w_i t), \quad (1)$$

where  $w_i$  is the ion drift velocity, determined from the time required for the ions to cross the drift space.

In the present experiment, we measure  $\alpha$  as a function of  $E/p$ , the ratio of the drift field to gas pressure. Results obtained in pure oxygen are shown in Fig. 1. It will be seen that for  $E/p > 3$  the quantity  $\alpha/p$  depends on  $E/p$  alone, while for  $E/p < 2$ ,  $\alpha/p$  increases linearly with  $p$  at each value of  $E/p$ . Results obtained in helium-oxygen mixtures, which extend to even lower  $E/p$  values, verify this pressure dependence down to near-thermal energies.

The quantity  $\alpha$  is related to the attachment frequency,  $\nu_a$ , by  $\nu_a = \alpha w_e$ , where  $w_e$  is the

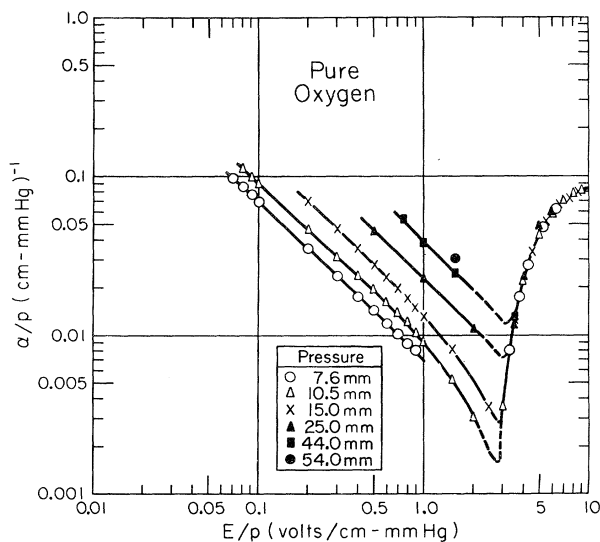


FIG. 1. Measured attachment coefficients ( $\alpha/p$ ) as a function of  $E/p$  for pure  $O_2$  at 300°K. Drift distances of 2.5 cm and 10 cm were used.

electron drift velocity. If electrons are lost by two-body collisions involving an electron and a neutral molecule (e.g., dissociative attachment) and by three-body collisions involving the electron, the molecule, and another molecule which stabilizes the reaction,<sup>7</sup> we may write for the time rate of change of electron density

$$dn_e/dt = -\nu_a n_e = -(\beta n + K n^2) n_e, \quad (2)$$

where  $\beta$  is the two-body attachment coefficient,  $n$  is the gas density, and  $K$  is the three-body coefficient.

The data of Fig. 1 are converted to values of  $\beta$  and  $K$  as functions of the average electron energy by the use of curves of electron drift velocity<sup>8</sup> and average electron energy<sup>9</sup> versus  $E/p$ . The results are shown in Figs. 2 and 3. The two-body coefficient,  $\beta$ , rises rapidly with average electron energy above  $\sim 1.3$  eV. As has been shown by Craggs *et al.*,<sup>10</sup> this process is the dissociative attachment reaction,  $O_2 + e \rightarrow O + O^-$ , observed in their beam experiments. The agreement concerning magnitude and energy depend-

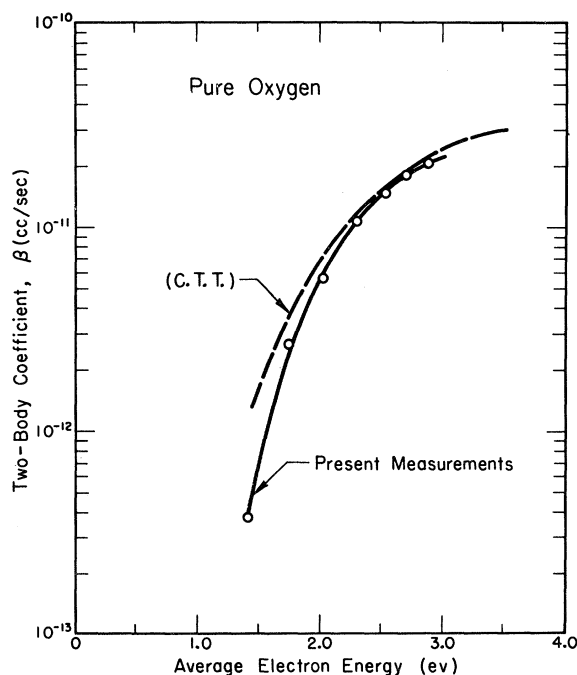


FIG. 2. Energy dependence of the two-body attachment coefficient. The dashed curve was obtained by averaging the cross sections measured by Craggs, Thorburn, and Tozer (C. T. T.) over a Druyvesteyn electron energy distribution for various average energies.

ence shown in Fig. 2 between our measurements (solid line) and an appropriate average over their data (dashed line) is within the uncertainties in the energy scale.

The three-body attachment coefficient observed at low electron energies is shown in Fig. 3. Earlier investigators appear to have missed this dependence because of large experimental errors<sup>1</sup> or because measurements were only made at a single pressure.<sup>2</sup> The data of Doehring fall within 20% of our 300°K curves from 0.7-1.0 eV. This three-body pressure dependence was recently independently identified by Hurst and Bortner,<sup>11</sup> who obtained data in N<sub>2</sub>-O<sub>2</sub> mixtures down to 0.35 eV. Their  $K$  values are approximately 10% lower than ours over the common energy range.

The helium-oxygen data<sup>12</sup> indicate a maximum in the  $K$  value for oxygen at average electron energies of ~0.08 eV for  $T_{\text{gas}} = 300^\circ\text{K}$  (0.04 eV) and at ~0.1 eV for  $T_{\text{gas}} = 77^\circ\text{K}$  (0.01 eV). The "thermal value" ( $T_{\text{gas}} = T_{\text{electron}} = 300^\circ\text{K}$ ) is approximately  $K = 2.8 \times 10^{-30}$  cm<sup>6</sup>/sec. This value leads to an attachment rate ~1000 times larger than

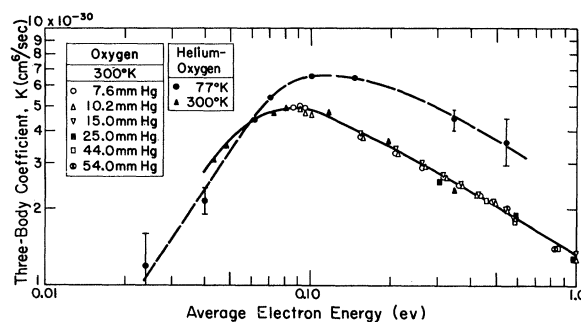


FIG. 3. Energy dependence of the three-body attachment coefficient for oxygen at 300°K and 77°K. The solid points were obtained from measurements of attachment coefficients in oxygen-helium mixtures containing 1-5% of oxygen.

that deduced from microwave studies of the oxygen afterglow<sup>5</sup> made at ~10 mm Hg pressure. The microwave results indicate a two-body attachment process. It has been suggested that the low microwave attachment rate is the result of substantial detachment of electrons during the afterglow occurring when vibrationally excited oxygen molecules produced during the microwave discharge strike negative ions.<sup>13</sup> In this case the final decay of electron density could occur at the rate of depletion of the vibrationally excited neutral molecules, leading to a low apparent attachment rate and a two-body type pressure dependence. Recent preliminary microwave afterglow studies<sup>14</sup> aimed at reducing this effect through the use of helium-oxygen mixtures yield attachment rates consistent with the drift tube studies.

A detailed discussion of the experimental results in terms of possible attachment processes and available theory<sup>7</sup> is rather lengthy and is deferred to a later article.

\* This work has been supported in part by an Air Force Special Weapons Center contract.

<sup>1</sup>N. E. Bradbury, Phys. Rev. **44**, 883 (1933).

<sup>2</sup>A. Doehring, Z. Naturforsch. **79**, 253 (1952).

<sup>3</sup>P. Herreng, Cahiers phys. **38**, 7 (1952).

<sup>4</sup>D. S. Burch and R. Geballe, Phys. Rev. **106**, 183 (1957).

<sup>5</sup>M. A. Biondi, Phys. Rev. **84**, 1072 (A) (1951); E. Holt, Bull. Am. Phys. Soc. Ser. II, **4**, 112 (1959); M. C. Sexton (private communication).

<sup>6</sup>For a summary of the attachment studies and of shutter designs, see L. B. Loeb, Basic Processes of Gaseous Electronics (University of California Press,

Berkeley, 1955).

<sup>7</sup>F. Bloch and N. E. Bradbury, Phys. Rev. **48**, 689 (1935). Other types of atoms or molecules may act as the third body. Mixture experiments in gases, such as He-O<sub>2</sub> and N<sub>2</sub>-O<sub>2</sub>, give *K* values for He and for N<sub>2</sub> as third bodies which are about 250 and 50 times smaller, respectively, than those for O<sub>2</sub>.

<sup>8</sup>These curves are an average of the data of H. L. Brose, Phil. Mag. **50**, 536 (1925); R. A. Nielsen and N. E. Bradbury, Phys. Rev. **51**, 69 (1937); R. W. Crompton (private communication); and P. Herreng, reference 3.

<sup>9</sup>These curves are an average of the data of R. H. Healey and J. W. Reed, The Behavior of Slow Electrons in Gases (Amalgamated Wireless, Sydney, 1951), p. 94 ff; H. L. Brose, Phil. Mag. **50**, 536 (1925); R. W. Crompton (private communication). We have taken the average energy to be equal to 1.5 times the

experimentally determined values of  $D/\mu$ .

<sup>10</sup>Craggs, Thorburn, and Tozer, Proc. Roy. Soc. (London) **A240**, 473 (1957).

<sup>11</sup>T. E. Bortner and G. S. Hurst, Health Phys. **1**, 39 (1958); G. S. Hurst and T. E. Bortner, Proceedings of the International Congress of Radiation Research, August, 1958 (to be published), and Phys. Rev. (to be published).

<sup>12</sup>Each point shown is derived from the slope of a plot of resultant *K* as a function of the fractional oxygen concentration at very low oxygen concentrations, e.g., 1-5%.

<sup>13</sup>J. D. Craggs, Third International Conference in Ionization Phenomenon in Gases, Venice, Italy, June, 1957 (The Italian Physical Society, October, 1957), p. 207.

<sup>14</sup>W. A. Rogers and M. A. Biondi (private communication).

## PROPOSAL FOR A METHOD OF POLARIZING 1-Mev DEUTERONS

Lee G. Pondrom

Aeronautical Research Laboratory, Wright-Patterson Air Force Base, Ohio

(Received March 5, 1959)

The purpose of this note is to point out that the elastic scattering of deuterons from He<sup>4</sup> can yield a rather large deuteron polarization with a high cross section. The differential cross section in *d*-He<sup>4</sup> elastic scattering has been measured to 3% or better in the region of 1-Mev incident deuteron energy.<sup>1</sup> The scattering in this region is characterized by a resonance at 1.070 Mev which corresponds to the formation of the first excited state of Li<sup>6</sup>, to which is given the assignment  $J=3^+$ .<sup>2</sup> If one uses the phase-shift analysis as calculated from these data assuming a single resonance level with  $J=3$ ,  $L=2$ ,<sup>2</sup> then one can construct the tensor invariants of the polarization for the scattered deuteron beam as a function of energy.<sup>3</sup> This is done by writing the scattered wave for incident spin projection  $m_s$  in the form

$$\psi(m_s) = \sum_{m_s'} a_{m_s'}^{m_s} \chi_{m_s'}^s, \quad (1)$$

where  $\chi_{m_s'}^s$  is an eigenvector of  $S_z$ , and  $a_{m_s'}^{m_s}$  is a coefficient involving the phase shifts and spherical harmonics. Here we choose the *z* axis in the incident direction, and the *y* axis normal to the scattering plane. Then the density matrix for the scattered beam is

$$\langle m_s' | \rho | m_s'' \rangle = (2s+1)^{-1} \sum_{m_s} a_{m_s'}^{m_s} a_{m_s''}^{m_s*}, \quad (2)$$

normalized such that  $\text{Tr}\{\rho\} = d\sigma/d\Omega = I_0$ . Following reference 3, we express the density matrix in terms of the unit matrix plus five independent tensor invariants:

$$\rho = \sum_{JM} A_{JM} T_{JM}, \quad (3)$$

where  $T_{JM}$  transforms under rotation of the quantization axis like the spherical harmonic  $Y_M^J(\theta, \phi)$ . The expectation values  $\langle T_{JM} \rangle$  can be calculated from the general rule

$$\langle T_{JM} \rangle = I_0^{-1} \text{Tr}\{\rho T_{JM}\}, \quad (4)$$

once the density matrix is known in terms of the phase shifts.

Figure 1 shows the cross section,  $I_0$ , and Figs. 2 and 3 give the tensor invariants for the scattered wave, with the *z* axis as chosen above, as a function of the incident deuteron energy in the region of the resonance. Coulomb forces are included in the calculation. The definitions of the invariants as shown on the figures are the same as in reference 3. The curves are reliable only in the region near the resonance energy, because the approximation  $\tan \beta_2^3 = \Gamma/[2(E_0 - E)]$  was used for the resonant phase shift  $\beta_2^3$ .  $\langle T_{10} \rangle$  of course, vanishes because of parity conservation, and  $\langle S_x \rangle$  vanishes because of the choice of the *y* axis. Thus  $i \langle T_{11} \rangle = (\sqrt{3}/2) \langle S_y \rangle$ .